UNBONDED PRESTRESSED PANEL TENDON STRESSES AT IN-PLANE NOMINAL FLEXURAL STRENGTH

N.J. Brooke[1], G.D. Wight[2], A.P. Russell[1] and J.M. Ingham[3]

ABSTRACT

A series of in-plane tests on post-tensioned concrete wall panels with unbonded tendons are described. These tests were used to verify that tendon stresses at nominal flexural strength can be accurately predicted for concrete walls using an equation previously developed for post-tensioned concrete masonry walls. Testing showed that the equation gives more accurate prediction of tendon stress than current design methods used in New Zealand. A secondary objective was to examine the accuracy of "true" predictions of wall performance obtained by finite element analysis. Predictions of wall force-displacement response, tendon stress increase and concrete strain generally matched experimental data with acceptable accuracy. The experimental response of some walls was significantly influenced by the existence of a bedding layer with low stiffness, which could not be accurately modelled.

Introduction

In recent years there has been much interest in structures that combine the ability to resist significant earthquakes with the ability to self-centre after such events. These structures typically employ a rocking mechanism to accommodate post-elastic deformations and are exemplified by the structures and components tested during the PRESSS program (Priestley et al. 1999). The performance of the rocking mechanism is often enhanced by the use of post-tensioning tendons that are unbonded over at least some of their length. Leaving tendons unbonded reduces the likelihood of tendon yielding during an earthquake and thus enhances the self-centering ability of the structure, but also makes prediction of nominal strength more difficult. This paper describes an experimental and computational investigation of the prediction of nominal flexural strength of wall panels with unbonded tendons.

In-Plane Response of Walls with Unbonded Post-Tensioning

The in-plane response of a wall with unbonded post-tensioning tendons is summarised in Figure 1. A complete procedure for predicting the force-displacement response of such walls (focused on masonry walls) has been published previously (Laursen 2002). Figure 1(a) shows a prestressed wall subjected to a lateral force V, which is assumed to act at an effective height h_e. The wall has a length l_w, and is subjected to an axial load consisting of the effective prestress force P, and dead and live load axial forces N. Figure 1(b) shows the force-displacement response for this wall that occurs as the lateral force V is

---

[1] Postgraduate Researcher, Dept. of Civil & Environmental Engineering, The University of Auckland, New Zealand
[2] Design Engineer, Ductal®, VSL Australia Pty. Ltd.
[3] Associate Professor, Dept. of Civil & Environmental Engineering, The University of Auckland, New Zealand

increased. Various flexural limit states are marked on this force-displacement plot.

Before the application of a lateral force, the stress profile at the critical wall base section is uniform as shown in Figure 1(c). The first limit state is known as 'first cracking' and occurs when the axial stress reaches zero at one end of the wall as depicted in Figure 1(d).

After first cracking the stiffness of the wall decreases as the horizontal crack that formed at the tension edge of the wall extends across the full depth of the wall and the wall begins to rock. The serviceability limit state is defined as the point when the stress in the extreme compression fibre reaches kf'_c as shown in Figure 1(e), where k (symbol adopted in this study) is either 0.45 or 0.6 depending on the nature of loading (ACI 318-05; NZS 3101:2006).
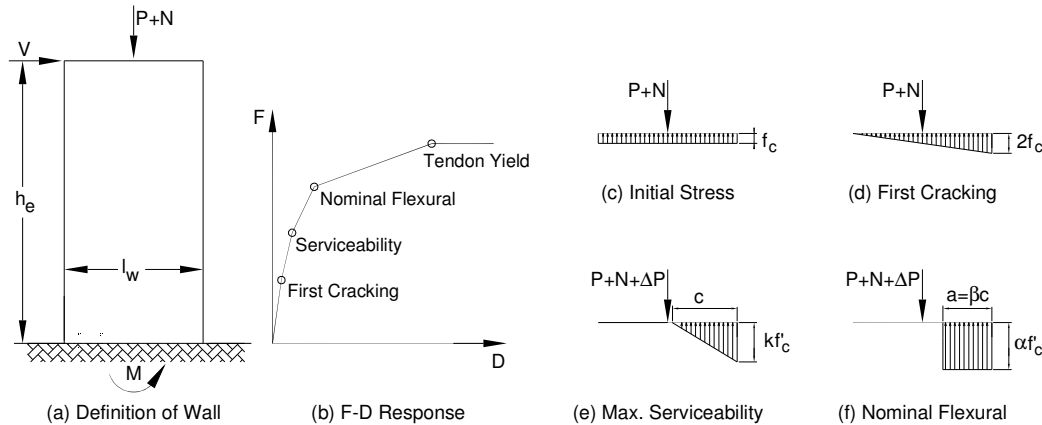

Figure 1.   Limit states for a post-tensioned wall.

Nominal flexural strength is defined as the strength when the strain at the extreme compression fibre reaches 0.003, being the code defined maximum usable strain. At this limit a rectangular stress block is assumed with a stress of $\alpha f'_c$ and a depth of βc, as shown in Figure 1(f). At this limit state significant rotation occurs at the horizontal base crack and the force in tendons located outside the compression zone increases beyond the initial effective force P. The prediction of this tendon force increase for walls loaded in-plane is the subject of this paper. In this paper the horizontal force required to develop this limit state is referred to as V_n.

Beyond nominal flexural strength, wall behaviour is dominated by rocking. Testing has shown that compression strains well in excess of 0.003 are achievable (Laursen 2002). Plastic hinges will form in the lower wall corners and the wall will rotate about these hinges. As the wall rotates, the force in the tendons and hence in-plane wall strength will increase until the tendons begin to yield. The force-displacement response shown in Figure 1(b) implies that all tendons yield at the same wall displacement. This will not be the case for walls with distributed tendons.

Predicting Unbonded Tendon Stresses at Nominal Strength

Accurate prediction of nominal flexural strength is an important part of structural design. For reinforced concrete and masonry members containing only bonded reinforcement nominal flexural strength can be predicted from a section analysis by assuming that plane sections remain plane and that there is strain compatibility between concrete and reinforcement. Predicting the strength of a member with unbonded reinforcement is more difficult. There is no requirement for strain compatibility between concrete and unbonded reinforcement at a section, and thus unbonded tendon stress change must be based on the average concrete strain along the unbonded length. This significantly complicates the exact calculation of tendon stress, and thus semi-empirical predictive equations are typically used for estimating tendon stresses at nominal flexural strength. Equations of this type which are found in New Zealand design

standards (NZS 3101:2006) were developed from experimental testing of beams (Mattock et al. 1971), and thus their suitability for use when designing walls is questionable.

Wight (2006) used a three stage method to investigate the accuracy of equations used to predict tendon stresses in masonry walls. The steps undertaken were:

- full scale masonry walls tested in the laboratory
- finite element model developed and verified against laboratory tests
- finite element analysis of 25 "virtual" walls used to determine tendon forces when masonry strain reached 0.003

Wight considered equations found in New Zealand (NZS 3101:2006; NZS 4230:2004), United States (MSJC 2005) and British (BS 5628-2:2000) design standards and found that none of the existing equations were able to accurately predict tendon stresses for all the walls analysed since the equations did not contain a sufficient number of variables. The equation found in New Zealand design standards is the same as that found in ACI 318. Based on the matrix of analysed walls Wight developed an improved equation for predicting tendon stresses in walls with unbonded tendons.

The Wight Equation for Predicting Unbonded Tendon Stresses

The stress in a post-tensioning tendon at nominal strength is given by the following equation:

$$f_{ps} = f_{se} + E_{ps}\Delta\varepsilon \leq f_{py} \tag{1}$$

where f_{ps} is the tendon stress at nominal strength, f_{se} is the initial tendon stress after losses, E_{ps} is the elastic modulus of the tendon and $\Delta\varepsilon$ is the change in tendon strain at nominal strength. To use Eq. 1 it is necessary to know the change in the tendon strain at nominal strength. The strain in the tendon is dependent on the rotation of the wall at nominal strength, which Wight (2006) showed was proportional to the wall aspect ratio divided by the wall axial stress ratio (the ratio of initial axial stress to concrete compressive strength). Based on this approximation, Wight suggested an equation for predicting tendon stresses at nominal strength, given here as Eq. 2.

$$f_{ps} = f_{se} + \left(\frac{\varepsilon_u \, h_e \, f_c' \, E_{ps}}{30 \, l_w \, f_c \, l_p}\right)\left[d_i - \left(\frac{f_c \, l_w}{\alpha\beta f_c'}\right)\right] \leq f_{py} \tag{2}$$

where ε_u is the assumed crushing strain of the concrete (typically 0.003), l_p is the unbonded length of the tendon, d_i is the distance between the extreme compression fibre and tendon centroid, and f_c is the initial stress in the wall from the effective prestress and axial load, which can be calculated as:

$$f_c = \frac{f_{se}A_{ps} + N}{l_w b_w} \tag{3}$$

where N is the axial load excluding prestress forces acting on the wall, A_{ps} is the total area of prestress tendons and b_w is the width of the wall. The coefficient in Eq. 2 (1/30) was chosen to provide the best fit to the data used to verify the equation.

To estimate the flexural strength of a wall, the stress in each tendon should be calculated separately, since tendon elongation is related to distance from the neutral axis. Wight has previously shown that for masonry walls, Eq. 2 provides a better estimate of tendon stress increase than current design equations (BS 5628-2:2000; NZS 4230:2004; MSJC 2005) for a range of wall aspect and axial force ratios.

Unbonded Tendon Stresses in Prestressed Concrete Wall Panels

This paper provides further verification of Wight's tendon stress equation by addressing two areas not covered in the original development:

- Although it was suggested that Eq. 2 was suitable to predict tendon stresses in concrete walls (Wight 2006), testing was not conducted to verify this assertion.
- Due to the highly non-homogenous properties of masonry it was not possible to determine experimentally the point when the masonry compression strain reached 0.003.

To provide information on these aspects of prestressed wall behaviour two concrete wall panels were constructed and tested at the University of Auckland.

Panel Design

Figure 2 shows details of the two wall panels constructed for this study. The panels were designed to have quite different aspect ratios to enable the effect of this variable on tendon stress to be considered. The walls contained straight plastic ducts that allowed unbonded post-tensioning tendons to be added as required. Wall A (aspect ratio 3.3) had three tendon ducts, while wall B (aspect ratio 1.5) had 5 tendon ducts. Tendon ducts were spaced at 406.4 mm (16 inch) centres to match the spacing of anchorage points in the laboratory. Both panels were constructed from an ordinary ready-mix concrete provided by Firth Industries that had a compressive strength at the time of testing of 33 MPa.

The walls were prestressed with high strength steel bars. These bars had a nominal diameter of 15 mm and measured yield strength of approximately 1050 MPa. The elastic modulus of the tendons was measured as approximately 190 GPa. An important parameter for estimating the stress in unbonded tendons is the length over which the tendon is unbonded. The unbonded length of tendons for walls A and B was taken as equal to the wall height plus 550 mm, which allowed for the thickness of the strong floor to which the walls were anchored and the height of the load cells used to measure the tendon stresses.

Experimental Method

The aim of this study was only to determine tendon stresses at nominal flexural strength and thus the wall panels were loaded monotonically using a test setup shown in Figure 2. In addition to simplifying testing, monotonic loading confined damage during testing to the compressed corner at the base of the wall. Thus by testing in both directions and then turning the wall upside down each panel could be used for four tests with different numbers of tendons and different initial stress levels. This greatly increased the quantity of data obtained from each test specimen. Table 1 gives information on the different configurations in which the walls were tested. The stress ratios used were lower than intended since the concrete strength was higher than anticipated. For prestressed walls the axial stress ratio would typically be in the range 0.05-0.25, and it can be seen in Table 1 that the stress ratios used were at the lower end of or outside this range. Note that the initial tendon stress levels given in Table 1 are ideal values (targets) while the initial axial stress in the wall and the predicted horizontal force required to cause a concrete compressive strain of 0.003 (V_n) were calculated from initial tendon stresses measured during each test. V_n was calculated based on the wall geometries seen in Figure 2 and tendon stress changes calculated according to Eq. 2.

Strain Measurement in Compressed Concrete

A key aim of the testing described in this paper was to determine experimentally when the extreme concrete fibre reached a compression strain of 0.003. Accurate measurement of strain close to the contact point of a rocking structure is affected by three difficulties:
- It is known that strain decreases exponentially with distance from the rocking interface. Since all practical instruments for measuring strain have a finite length, any strain measured will be an average and thus less than the peak strain within the gauge length.

- Choice of instrumentation involves compromise between cost, gauge length and gauge location. Re-useable displacement transducers have the lowest cost but typically a long gauge length, while strain gauges mounted on embedded reinforcement have a small gauge length but are difficult to place close to the extreme compression fibre. Strain gauges mounted directly on the concrete surface provide the most realistic measurement of local concrete strains, but must have a longer gauge length than gauges mounted on steel to accommodate the non-homogeneous nature of concrete
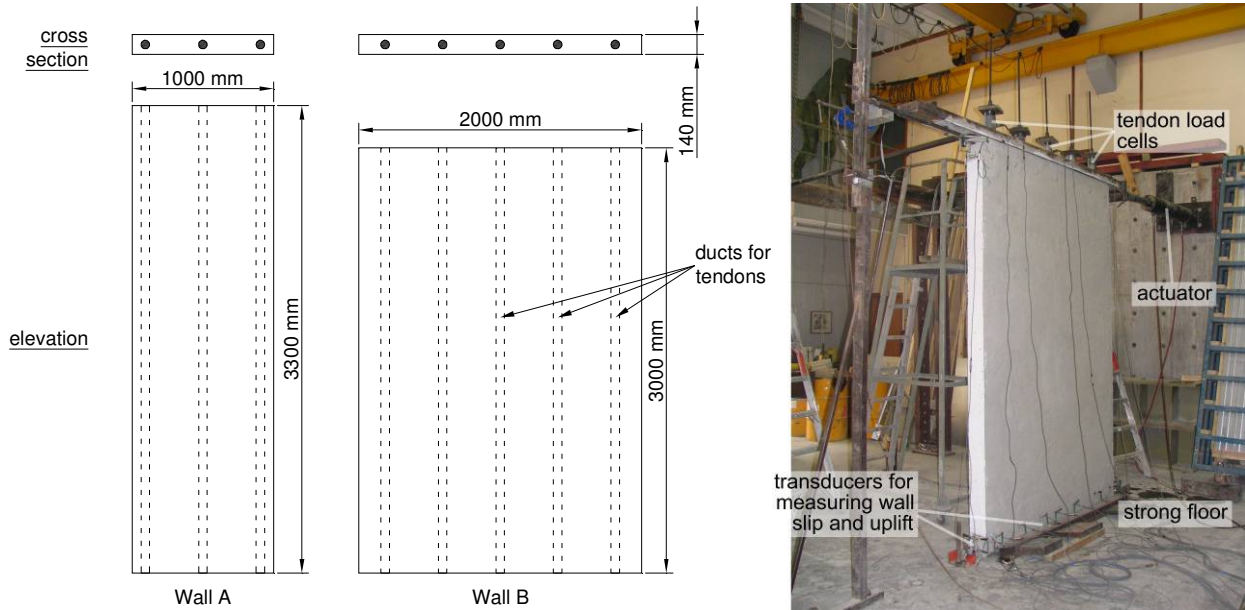- The contact surfaces at the rocking interface can significantly affect local strain readings.

Figure 2.   Elevation and cross section of wall panels and test setup.

Table 1.   Prestressing configurations for walls A and B.

Wall	Configuration	Tendons Stressed	Initial Tendon Stress (MPa)#	Wall Axial Stress Ratio*	V_n (kN)*
A	i	1, 2, 3	440	0.056	54.1
	ii	1, 2, 3	616	0.079	63.1
	iii	1, 3	440	0.038	46.0
	iv	2	440	0.020	26.8
B	i	1, 2, 3, 4, 5	616	0.062	218.0
	ii	1, 2, 3, 4, 5	440	0.044	188.4
	iii	2, 4	352	0.016	112.1
	iv	2, 4	616	0.026	117.0

nominal value   * based on tendon forces measured at beginning of test

During testing of the first wall panel (wall B) a number of problems with the test setup were encountered that prevented useful strain measurements from being recorded. Wall B was initially installed with no bedding layer between the strong floor and the wall base, which was done to prevent the properties of the bedding layer from influencing wall response. Initial testing demonstrated that a bedding layer was

required as full contact was not achieved under the toe of the wall. Placing a layer of cement mortar under the wall allowed full contact at the rocking interface, but the lower stiffness of this layer had a significant influence on wall force-displacement response. In addition to these problems no useable strain data was obtained from wall B since no strain gauges were installed on the concrete surface and other instrumentation employed proved unable to measure concrete strain at the extreme compression fibre.

Based on the problems found when testing wall B, two improvements were made to the test and instrumentation setup before testing of wall A commenced. High strength gypsum plaster was used instead of cement based mortar to reduce the influence of the bedding layer on the experimental results. To improve strain readings from the extreme compression fibre three strain gauges were surface mounted on the concrete in this region. These gauges had a length of 30 mm and were centered 30 mm, 130 mm and 430 mm above the base of the wall.

Experimental Results

Figure 3 and Figure 4 show the experimental force-displacement responses obtained from testing the four configurations of walls A and B respectively. Also shown are force-displacement predictions generated by the finite element analysis program Abaqus. These predictions were obtained using a model developed prior to testing (Wight 2006), and are therefore true predictions.
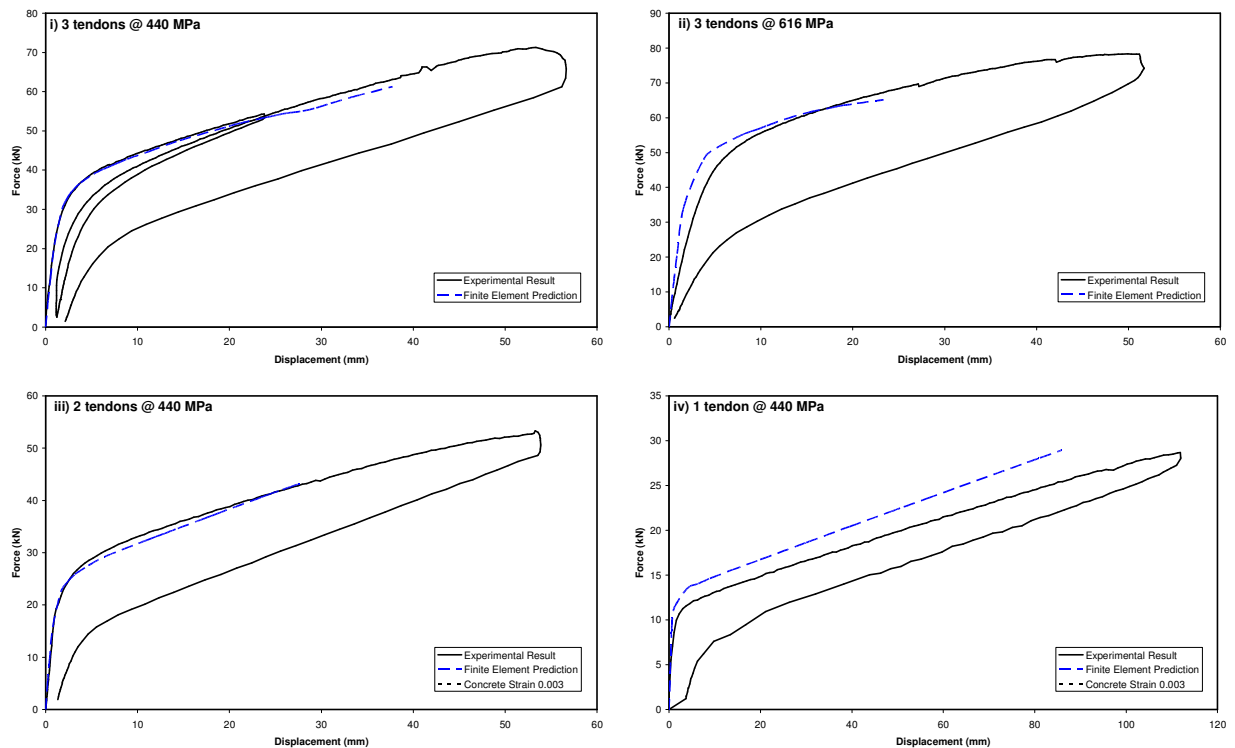

Figure 3.   Force displacement responses for wall A configurations.

With the exception of configuration (iv), the force-displacement response of wall A was predicted with acceptable accuracy. It is not clear why the finite element model was unable to accurately predict the response of configuration (iv). This configuration had a very low axial stress ratio (see Table 1) and thus the neutral axis depth of the wall was small relative to the finite element size used. It is thought this may have impacted on the accuracy of prediction. An attempt was made to reduce the finite element size in the vicinity of the compressed toe of the wall, but this resulted in problems with solution convergence.

Figure 4 shows the force-displacement response of wall B configurations (ii) and (iv). No force-displacement response is shown for configuration (i) as a number of problems occurred during testing of this wall which rendered the test data useless, while configuration (iii) is omitted here due to space limitations. The finite element model overestimated the force-displacement response for wall B. The experimental force-displacement response of the wall was strongly influenced by the soft mortar bedding layer placed between the wall and the strong floor. It proved impossible to include the influence of this soft layer in the finite element model, and thus the stiffness of the walls was significantly overestimated by the finite element model. As previously stated, the influence of the bedding layer was removed during testing of wall A by using high strength gypsum plaster rather than cement mortar as a bedding material. Since the effect of foundation material on the response of rocking walls is obviously significant, this could be an area that warrants further investigation if it is considered likely that such soft foundation layers might be encountered in practice.
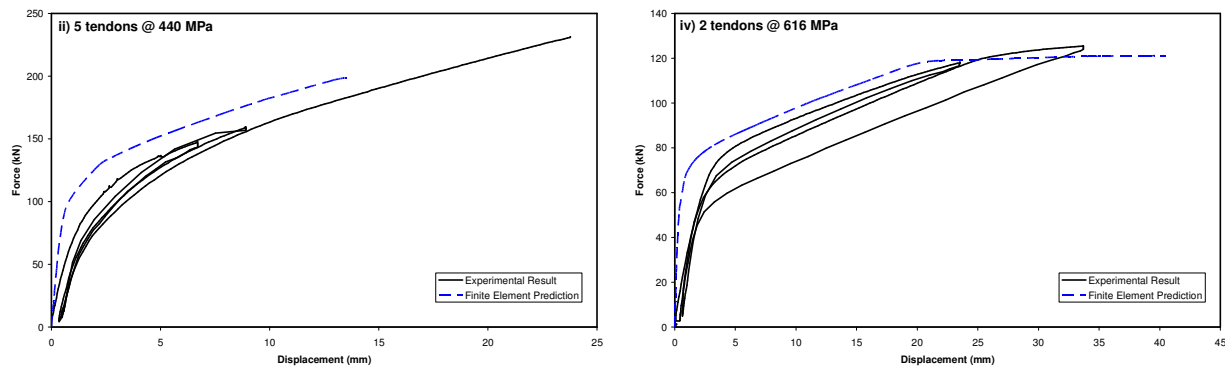

Figure 4.   Force displacement responses for wall B configurations (ii) and (iv).

Concrete Strain at the Extreme Compression Fibre

Figure 5 shows concrete compression strain plotted against applied horizontal force for the four configurations of wall A. Experimental strains were measured by strain gauges with a gauge length of 30 mm, centered 30 mm above the base of the wall, while the strains predicted by finite element analysis are the average strain in the lowest finite element (element size 50 mm for configurations (i), (ii) and (iii) and 25 mm for configuration (iv)). Note that experimental results in Figure 5 are abbreviated compared to those in Figure 3. The reason for this is that the strain gauge readings shown in Figure 5 were distorted as concrete crushing and spalling started to occur, and thus results beyond those shown below are meaningless.

The agreement between experimental and analytical results is excellent for configurations (i) and (ii), acceptable for configuration (iii) and poor for configuration (iv). The poor correlation found for configuration (iv) reflects the difficulty encountered in modeling the force-displacement response and the problems that are believed to be attributable to the low axial stress ratio.

For configurations (iii) and (iv) concrete strains of 0.003 were not measured experimentally or predicted by finite element analysis despite crushing being observed experimentally. The neutral axis depth of configurations (iii) and (iv) was small due to the low prestress levels used, and thus the exponential strain decrease mentioned previously occurred over a very short distance, reducing the average strain measured over the gauge lengths used in this study. Thus it is not possible to state the nominal flexural strength of configurations (iii) and (iv) of wall A based on experimental or finite element analysis data.
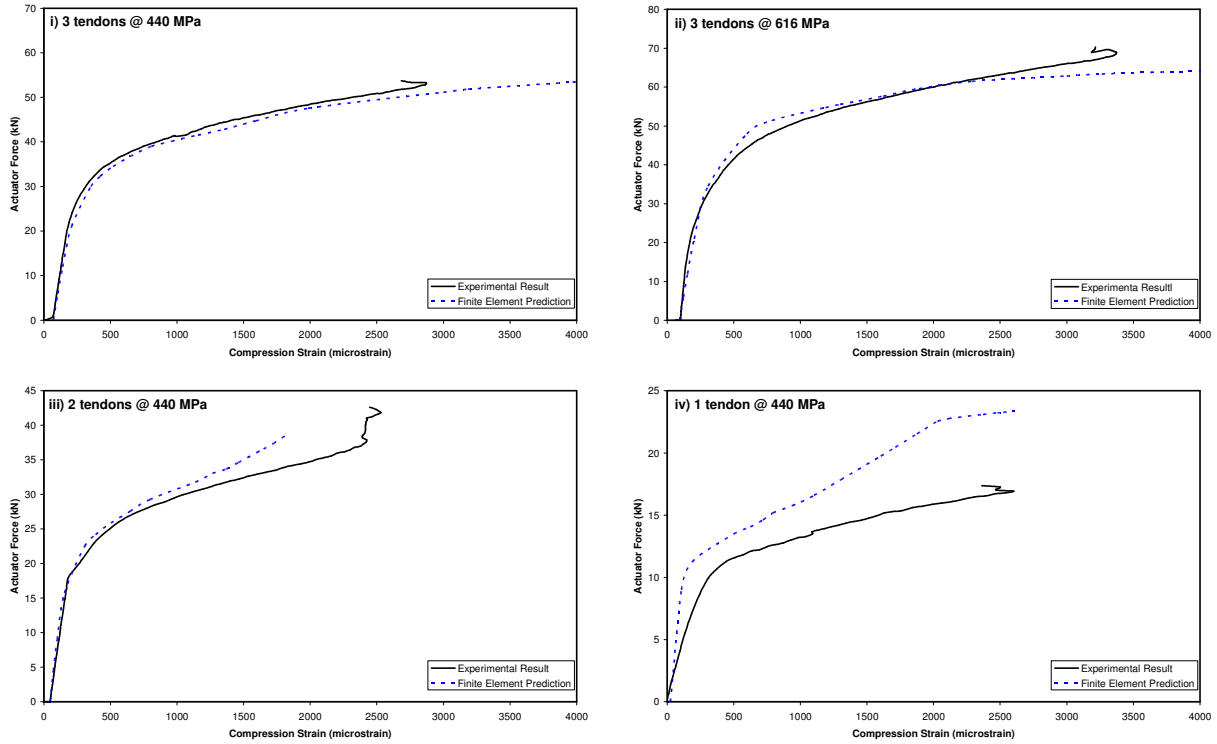
Figure 5.   Comparison of experimental and computational force-strain response.

Tendon Stresses in Concrete Wall Panels

Figure 6 shows the tendon force-wall displacement responses obtained from configurations (i) and (iii) of wall A. These are compared to similar responses obtained by finite element analysis. It can be seen that the prediction of tendon stresses is acceptable, although finite element analysis appears to over-estimate tendon stress.
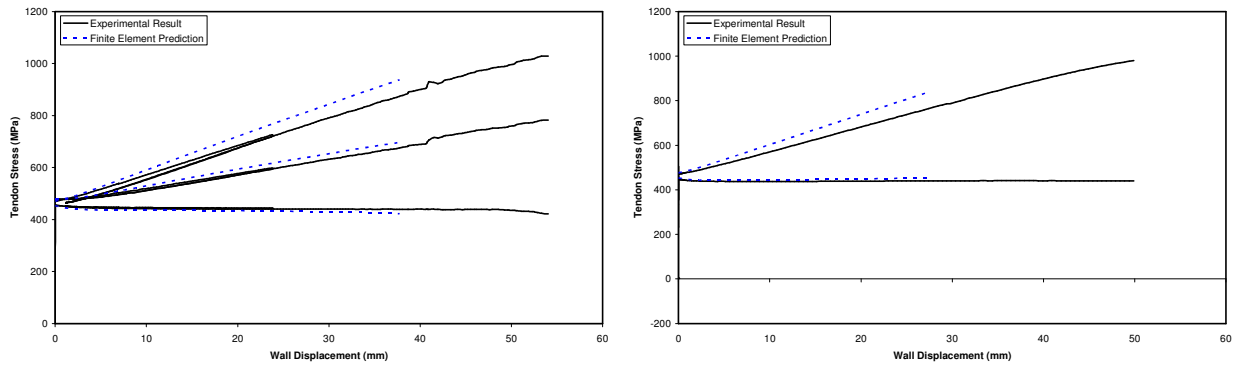

Figure 6.   Comparison of actual and predicted tendon stresses for wall A (i) (left) and A (iii) (right).

The focus of this paper is to accurately predict wall strength when a concrete strain of 0.003 occurs at the extreme compression fibre. To predict this strength it is necessary to accurately predict tendon stresses when this concrete strain occurs. Of the eight wall tests described in this paper, concrete strains of 0.003 were measured in only two tests. These two tests are the focus of Figure 7, which compares tendon stresses coincident with a concrete strain of 0.003 obtained experimentally and similar strains predicted by finite element analysis, Eq. 2 and the design equation currently found in NZS 3101. It can be seen that

finite element analysis has accurately predicted the tendon stress change in all six tendons. Eq. 2 has predicted the tendon stress change accurately with the exception of one tendon, while the equation currently used for design tends to overestimate tendon stress change in tendons close to the neutral axis, and underestimate stress change in tendons distant from the neutral axis. When considered in terms of total tendon stress at nominal flexural strength, it is evident that Eq. 2 accurately predicts all tendon stresses, with the greatest error being around 7%.
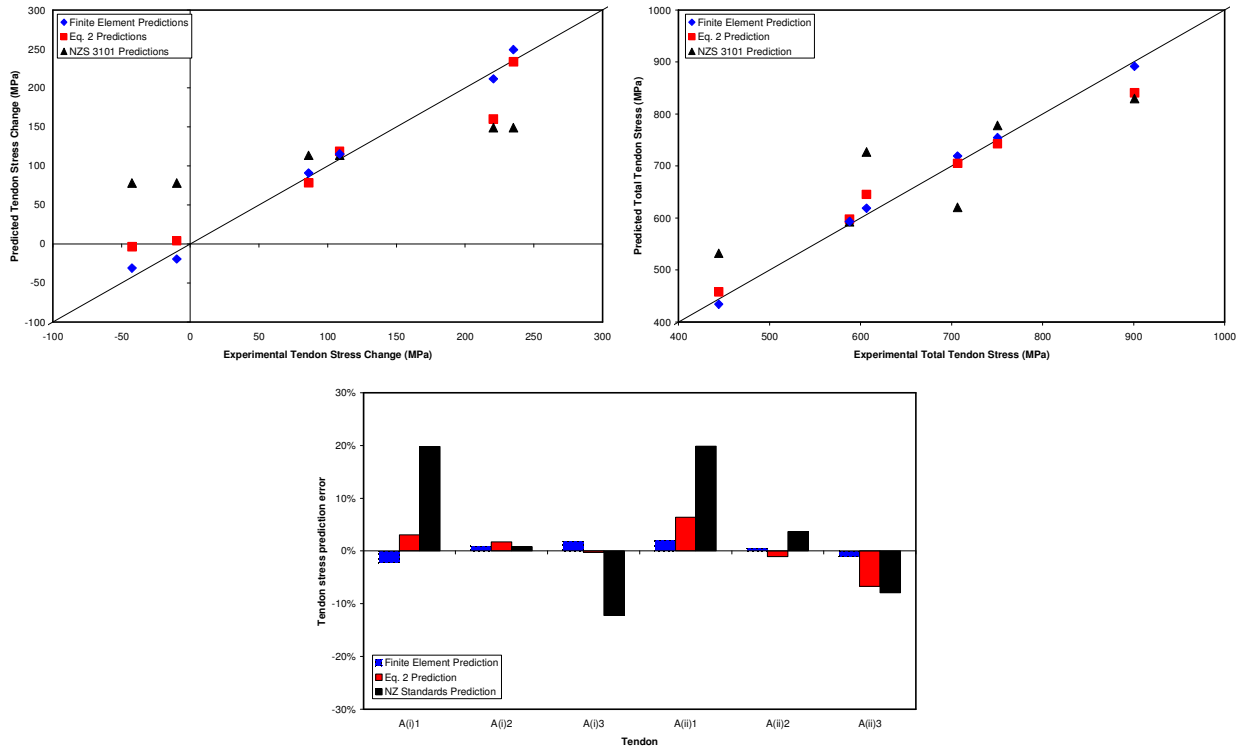

Figure 7.   Comparison of tendon stress predictions at nominal flexural strength for Wall A configurations (i) and (ii).

Flexural Strength Prediction Based on Eq. 2

Having shown that Eq. 2 can accurately predict tendon stresses at nominal flexural strength it is of interest to compare the experimental strength of the wall when a concrete strain of 0.003 occurs with the strength predicted by finite element analysis and by hand calculation based on a rectangular stress block and tendon stresses predicted by Eq. 2. This comparison is shown in Table 2.

For wall A only configurations (i) and (ii) are shown in Table 2. As stated previously, neither experimental nor finite element strain readings reached 0.003 and thus no nominal flexural strength could be established for these configurations. The experimental, finite element and hand calculation results for configurations (i) and (ii) are in close agreement, with finite element analysis underestimating wall strength by a maximum of 12%. This close agreement between finite element analysis and experimental results suggests it is appropriate and meaningful to compare the flexural strengths for wall B predicted by finite element analysis and hand calculations, despite there being no way of stating what the nominal strength was experimentally due to a lack of appropriate strain readings. Hand calculation accurately predicts the strength of all walls with the exception of wall B configuration (iii). This configuration had a very low axial stress ratio which was outside the range considered during development of Eq. 2 (Wight 2006).

Table 2.   Comparison of Measured and Predicted Wall Nominal Flexural Strength.

Wall	Configuration	Experimental V_n	FEA V_n	Eq. 2 V_n	Eq. 2/FEA
A	i	57.7 kN	51.2 kN	50.2 kN	0.98
A	ii	66.7 kN	62.9 kN	59.3 kN	0.94
B	i	-	225.9 kN	214.6 kN	0.95
B	ii	-	186.4 kN	185.0 kN	0.99
B	iii	-	92.9 kN	108.8 kN	1.17
B	iv	-	108.6 kN	113.6 kN	1.05

Conclusions

This paper has discussed a series of tests on concrete wall panels reinforced with unbonded post-tensioning. The tests were conducted to verify a previously proposed equation for predicting tendon stress at nominal flexural strength for masonry walls with unbonded tendons (Wight 2006). It has been shown that the proposed equation gives more accurate prediction of tendon stresses than the equation currently used for design in New Zealand.

A finite element model developed for concrete masonry walls was used to predict the behaviour of the walls described in this paper. It has been shown that the stiffness of the bedding layer placed between a wall and its foundation has a significant effect on its force-displacement response. Difficulties modeling this flexible layer prevented accurate finite element modeling of some wall tests. Where the influence of the bedding layer was eliminated wall force-displacement response was predicted with acceptable accuracy, as was the change of tendon stress and concrete strain with wall displacement.

References

ACI 318-05, *Building Code Requirements for Structural Concrete*. American Concrete Institute, Farmington Hills, Michigan.

BS 5628-2:2000, Code of Practice for the use of Masonry. Part 2: Structural Use of Reinforced and Prestressed Masonry. British Standards Institution, London, U.K.

Laursen, P. T., 2002. Seismic Analysis and Design of Post-tensioned Concrete Masonry Walls, *PhD Thesis*, Dept. of Civil and Environmental Engineering, University of Auckland, New Zealand.

Mattock, A. H., J. Yamazaki and B. T. Kattula, 1971. Comparative Study of Prestressed Concrete Beams, with and without Bond, *Proc. ACI Journal* 68(3), 116-125.

MSJC, 2005. *Building Code Requirements for Masonry Structures*. ACI 530-05/ASCE 5-05/TMS 402-05, Masonry Standards Joint Committee, USA.

NZS 3101:2006, *Concrete Structures Standard*. Standards New Zealand, Wellington, New Zealand.

NZS 4230:2004, *Design of Reinforced Concrete Masonry Structures*. Standards New Zealand, Wellington, New Zealand.

Priestley, M. J. N., S. Sritharan, J. R. Conley and S. Pampanin, 1999. Preliminary Results and Conclusions from the PRESSS Five-Story Precast Concrete Test Building, *PCI Journal* 44(6), 42-67.

Wight, G. D., 2006. Seismic Performance of a Post-Tensioned Concrete Masonry Wall System, *PhD Thesis*, Dept. of Civil and Environmental Engineering, University of Auckland, New Zealand.